

## Analytic approach to the antiferromagnetic van Hove singularity model for high- $T_c$ superconductors

D. Y. Xing

*National Laboratory of Solid State Microstructures and Department of Physics, Nanjing University, Nanjing 210093, China*

Mei Liu and Yong-Gang Wang

*Department of Physics and Laboratory of Molecular and Biomolecular Electronics, Southeast University, Nanjing 210096, China*

Jinming Dong

*National Laboratory of Solid State Microstructures and Department of Physics, Nanjing University, Nanjing 210093, China*

(Received 7 April 1999)

An analytic approach to the antiferromagnetic van Hove singularity (VHS) model is developed to account for the small oxygen-isotope effect of high- $T_c$  cuprates. Starting from the hole dispersion in an antiferromagnetic background, we derive and obtain analytic expressions for density of states (DOS) with a narrow VHS peak. Both  $T_c$  and the isotope coefficient  $\alpha$  are calculated using the hole-boson coupling and  $d$ -wave gap equation. It is shown that a very small  $\alpha$  at optimal doping stems from the fact that the half-width of the VHS peak in the DOS is smaller than the maximal boson energy. The origin of  $\alpha$  varying with doping is also discussed. [S0163-1829(99)00134-4]

### I. INTRODUCTION

It has been widely accepted that owing to layered structures of Cu oxides, carriers within the  $\text{CuO}_2$  planes exhibit two-dimensional (2D) nature of electron dynamics. One-electron band-structure calculations<sup>1</sup> showed that the Cu oxides are characterized by 2D Fermi-surface nesting. As a result, following the discovery of the high- $T_c$  superconductors, the van Hove singularity (VHS) in density of states (DOS) was proposed as a  $T_c$ -enhancement mechanism for them.<sup>2</sup> However, the idea of achieving high- $T_c$  superconductivity with the aid of a sharp peak in DOS at the Fermi energy  $E_F$  along with a phonon-mediated pairing was not widely accepted. The main objections to this high- $T_c$  mechanism mostly stem from the fact that its effectiveness in enhancing  $T_c$  depends on the restriction of  $E_F$  being at or very close the VHS, but at that time there was no convincing experimental evidence for a DOS singularity near  $E_F$ . Furthermore, the phonon-mediated pairing mechanism raises doubts in the consideration of very small oxygen-isotope effect<sup>3</sup> (i.e.,  $\alpha \approx 0-0.2$ ,  $T_c \propto M^{-\alpha}$ , where  $M$  is the atomic mass of oxygen) observed in the cuprates with optimal doping.

The VHS model reinvented in 1990 by Tsuei *et al.*<sup>4</sup> to account for the doping dependence of the oxygen-isotope mass exponent  $\alpha$  observed experimentally in  $\text{La}_{2-x}\text{Sr}_x\text{CuO}_4$  (LSCO) (Ref. 5) and  $\text{YBa}_2\text{Cu}_3\text{O}_{7-x}$  (YBCO).<sup>6</sup> Since then the van Hove scenario of the high- $T_c$  cuprates has forged rapidly ahead. First, high-resolution angle-resolved photoemission spectroscopy (ARPES) experiments<sup>7,8</sup> suggested that an extended region of flat  $\text{CuO}_2$  derived band close to  $E_F$  exists for YBCO as well as other high- $T_c$  cuprates with optimal doping, providing a strong support for the concept of VHS in DOS. Second, band-structure calculations<sup>9</sup> indicated

that there is a VHS near  $E_F$  in the Hg-based cuprates ( $\text{HgBa}_2\text{Ca}_{n-1}\text{Cu}_n\text{O}_{2n+2+\delta}$ ) for  $n=0, 1$ , and 2. By varying the dopant level  $\delta$ , the location of  $E_F$  can be moved to coincide with the VHS. The calculated values of  $\delta$  needed to achieve the van Hove condition are in good agreement with the  $T_c$ -optimized composition reported in the literature,<sup>10</sup> strongly supporting the existence of VHS near  $E_F$  in these Hg cuprates. Third, the VHS model has been used to account for many anomalous superconducting and normal-state properties of high- $T_c$  cuprate superconductors, including the high- $T_c$  and reduced isotope effect,<sup>4,11,12</sup> the linearly temperature-dependent resistivity,<sup>13</sup> the specific-heat jump at  $T_c$ ,<sup>14</sup> the anomalous thermopower,<sup>15</sup> the thermal conductivity,<sup>16</sup> and the uniaxial stress effect on  $T_c$ .<sup>17</sup> Finally, the van Hove scenario has been developed well beyond the previous theoretical framework of the phonon-mediated  $s$ -wave pairing. It was found that the VHS in DOS can be caused not only by the 2D band structure,<sup>11</sup> but also by antiferromagnetic (AF) correlation effects in the  $\text{CuO}_2$  planes.<sup>18-20</sup> It is well known that strong correlations of electrons and their quasi-2D behavior are two most important features of the high- $T_c$  superconductors. Both of them are close related to the existence of VHS, indicating that good agreement between the VHS theory and the experiments is entirely by no accident.

Recently, the ‘‘antiferromagnetic van Hove’’ (AFVH) model was proposed by Dagotto and co-workers<sup>18-20</sup> that the flat band near  $E_F$  or the VHS in DOS comes from the AF correlation effects. Using the 2D  $t$ - $J$  model and the quantum Monte Carlo method, the dispersion of one hole in an AF background can be calculated accurately. At small  $J/t$ , the hole dispersion is given by  $\varepsilon_{\mathbf{k}} = 1.33J \cos k_x \cos k_y + 0.37J(\cos 2k_x + \cos 2k_y)$  with  $J = 0.125$  eV and strong correlation effects are included.<sup>19</sup> This dispersion relation of the

quasiparticle is similar to that derived from a 2D tight-binding band structure in which the hole moves only within the same sublattice to avoid distorting the AF background.

Earlier theoretical works on the van Hove scenario were based on the assumption of conventional  $s$ -wave pairing. Recently, the VHS theory has been extended to the  $d$ -wave case,<sup>18-22</sup> in which the pairing state is a highly anisotropic  $d_{x^2-y^2}$ -wave state. In the study of the pairing symmetry, a most important but unsolved problem is what kind of mechanism creates attractive interactions between holes. In the BCS theory the usual hole-boson interaction is favorable to the  $s$ -wave pairing. In the cuprate superconductors, destabilization of the  $s$ -wave pairing is caused by the presence of large on-site Coulomb repulsion. This large on-site repulsion is fatal in the  $s$ -wave channel, but it drops out of the  $d$ -wave gap equation. The driving force for the  $d$ -wave pairing is the attractive interactions between the holes on nearest-neighbor sites. A most plausible candidate is the AF superexchange  $J$ ,<sup>18,19</sup> which is known to be a huge effect ( $J \sim 120$  meV) in the undoped insulators. However, while many numerical studies suggested that the small AF correlation can substantially affect the quasiparticle dispersion (single-particle Green's function), it has not been shown that it can also lead to pairing (two-particle Green's function, with hole Coulomb repulsion included). Thus Nazarenko and Dagotto<sup>20</sup> recently proposed a mixed phononic and electronic model where phononic pairing occurs between holes that are strongly dressed by AF fluctuations. Although the hole-phonon coupling is much smaller than in normal metals, the large DOS of dressed holes boosts  $T_c$  to realistic values. Their numerical calculations yield an oxygen-isotope coefficient that is small at optimal doping but becomes close to the BCS value 0.5 in the underdoped and overdoped regimes.

Since the AFVH model used to be solved numerically, the physical reason has not yet been clearly known why the hole dispersion used in Ref. 20 is able to result in a very small isotope coefficient  $\alpha$  at optimal doping and an increasing  $\alpha$  with  $E_F$  away from the VHS. In this paper we first derive analytically the DOS of the AFVH model with the dispersion of Eq. (1) and then use the hole-boson coupling and  $d$ -wave gap equation to calculate  $T_c$  and the isotope coefficient. It is shown that the prefactors of two terms in the dispersion, in particular the ratio between them, have important effects on the DOS, and the narrow van Hove peak in DOS plays a critical role in reducing  $\alpha$  and enhancing  $T_c$ . From the analytical result for the isotope coefficient, we find that when the half-width of the van Hove peak in the DOS is smaller than the maximal boson energy, a very small  $\alpha$  can be obtained at optimal doping. The origin of  $\alpha$  varying with doping is also discussed.

## II. DENSITY OF STATES

Starting from the 2D  $t$ - $J$  model and using the quantum Monte Carlo method, the hole dispersion in an AF background at half-filling was obtained. It is approximately valid also at finite doping.<sup>20</sup> If using the electronic language, we write the dispersion as

$$E_{\mathbf{k}} = -2t_2[2 \cos k_x a \cos k_y a + (\gamma/2)(\cos 2k_x a + \cos 2k_y a)], \quad (1)$$

where  $\gamma$  was taken to be different values:  $\gamma = 1.53$ ,<sup>18</sup> 1.113,<sup>19</sup> and 1.055,<sup>20</sup> and  $a$  is the lattice constant. As will be shown below, its reasonable value taken is very important in the AFVH model. This dispersion relation of the quasiparticle can be regarded as coming from a 2D tight-binding band model, in which  $t_2$  and  $t_3 = \gamma t_2/2$  are the hopping integrals between second- and third-nearest-neighbor Cu sites on the  $\text{CuO}_2$  plane, respectively, but the nearest-neighbor hopping is absent because the hole moves within the same sublattice to avoid distorting the AF background. Making changes of variables into  $p_x = (k_x + k_y)/\sqrt{2}$ ,  $p_y = (k_x - k_y)/\sqrt{2}$ , and  $b = \sqrt{2}a$ , we have  $E_{\mathbf{p}} = 2t_2 W_{\mathbf{p}}$  for a quasielectron where

$$W_{\mathbf{p}} = -\cos p_x b - \cos p_y b - \gamma \cos p_x b \cos p_y b. \quad (2)$$

This result looks like that obtained from a 2D tight-binding model for a sublattice of the AF background by taking into account nearest-neighbor and next-nearest-neighbor hopping integrals, the unit-cell area of the sublattice being  $b^2 = 2a^2$  and the corresponding Brillouin zone (BZ) rotated by  $\pi/4$ . According to the Green's-function approach,<sup>23</sup> the electronic DOS is associated with the imaginary part of the single-particle Green's function  $G(E, \mathbf{p})$  by

$$N(E) = \frac{1}{\pi} \sum_{\mathbf{p}} \text{Im} G(E, \mathbf{p}), \quad (3)$$

where  $G(E, \mathbf{p}) = (E - E_{\mathbf{p}} - i0^+)^{-1}$  with  $0^+$  a positive infinitesimal. From Eq. (3) the electronic DOS is given by

$$N(E) = \frac{b^2}{\pi^2} \int_0^{\pi/b} dp_x \int_0^{\pi/b} dp_y \delta(E - 2t_2 W_{\mathbf{p}}). \quad (4)$$

Making changes of integral variables into  $u = \cos p_x b$ ,  $v = \cos p_y b$  and setting  $w = -u - v - \gamma uv$ , we can rewrite Eq. (4) as

$$N(E) = \frac{1}{2t_2 \pi^2} \int_{-1}^1 dv \int_{-1}^1 du \frac{\delta(\varepsilon - w)}{\sqrt{1-u^2} \sqrt{1-v^2}}, \quad (5)$$

where  $\varepsilon = E/(2t_2)$ , and the integral region is confined within a square ( $-1 \leq u \leq 1$ ,  $-1 \leq v \leq 1$ ). To perform integral over  $u$  using the  $\delta$  function, we change further the integral variables into  $v$  and  $w$ , and so Eq. (5) becomes

$$N(E) = \frac{1}{2t_2 \pi^2} \iint \frac{dv dw \delta(\varepsilon - w)}{\sqrt{1-v^2} \sqrt{(1+\gamma v)^2 - (w+v)^2}}. \quad (6)$$

Here, owing to  $\gamma > 1$ , the integral regions of  $v$  and  $w$  are found to have a more complex pattern than in the case of  $\gamma \leq 1$ , as shown in Fig. 1(a). For ease of understanding the integral regions, we plot isoenergetic lines on the 2D BZ ( $-\pi/b \leq p_x, p_y \leq \pi/b$ ) in Fig. 1(b). For the region of  $\varepsilon \leq 2 - \gamma$ , the lowest energy  $\varepsilon = -2 - \gamma$  corresponds to  $\Gamma$  point in the BZ; with increasing energy, the isoenergetic circle enlarges and becomes gradually square. As the energy is increased to  $\varepsilon = 2 - \gamma$ , besides the squarish circle, the isoenergetic line also includes four vertexes of the BZ, corresponding to the point  $(v, w) = (-1, 2 - \gamma)$  in Fig. 1(a). For the region of  $2 - \gamma \leq \varepsilon < 1/\gamma$ , each isoenergetic line consists of two parts: an approximate square with round corners and four arcs around the corners, shown by the dashed lines

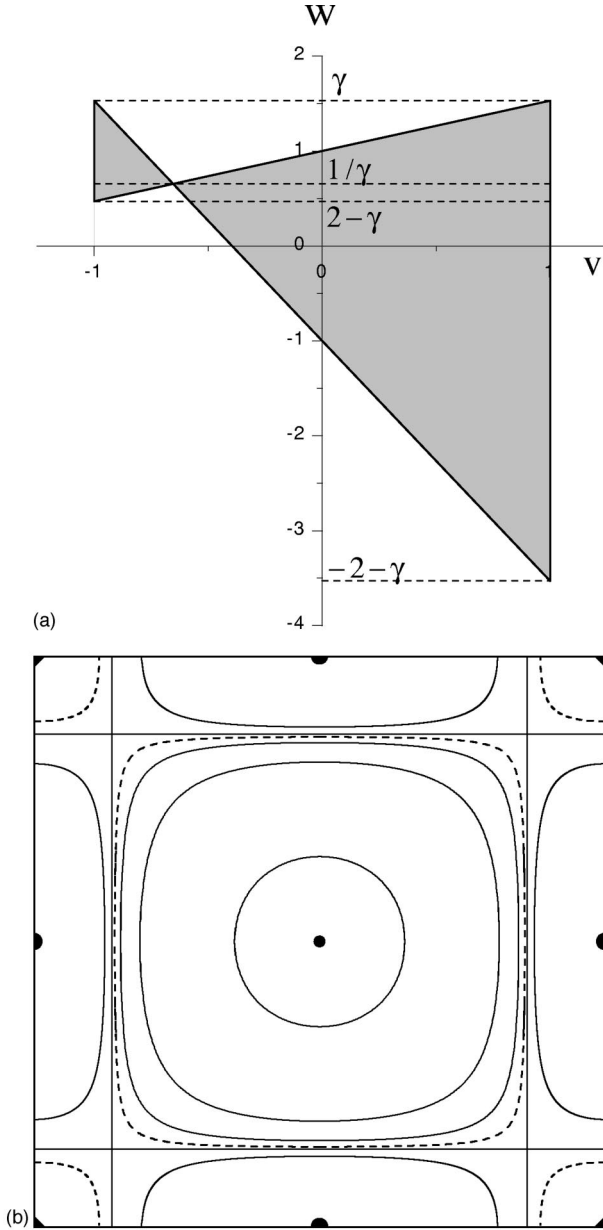


FIG. 1. (a) Integral region of  $v$  and  $\varepsilon$  in Eq. (6) is shown as the shaded area. It can be divided into three energy ranges:  $-2 - \gamma \leq \varepsilon \leq 2 - \gamma$ ,  $2 - \gamma \leq \varepsilon \leq 1/\gamma$ , and  $1/\gamma \leq \varepsilon \leq \gamma$ . (b) Isoenergetic lines of quasielectron dispersion [Eq. (2)]. From inside to outside,  $\varepsilon_{\mathbf{k}}$  is successively equal to  $-2 - \gamma$  (center point),  $-2.5$ ,  $0$ ,  $2 - \gamma$ ,  $0.6$  (dashed lines),  $1/\gamma$  (four straight lines),  $0.8$ , and  $\gamma$  (four points). The only parameter taken is  $\gamma = 1.53$  (Ref. 18).

in Fig. 1(b). In this energy range there are two integral regions; the approximated square in Fig. 1(b) corresponds to the right integral region in Fig. 1(a), while the four arcs correspond to the left integral region. At  $\varepsilon = 1/\gamma$ , the isoenergetic line consists of four straight lines with square crossing at  $|p_x| = |p_y| = \pi - \cos^{-1}(1/\gamma)$ . Evidently, a ideal nesting appears automatically in the AFVH model and it can be used to account for abnormal normal-state properties observed in the high- $T_c$  cuprate oxides. For the region of  $\varepsilon > 1/\gamma$ , the isoenergetic line evolves into four arcs centered around  $(p_x, p_y) = (0, \pm\pi)$  and  $(\pm\pi, 0)$ , respectively. Finally, at  $\varepsilon = \gamma$ , the isoenergetic line reduces to four points  $(0, \pm\pi)$  and  $(\pm\pi, 0)$ .

In Eq. (6), the integral over  $w$  is readily performed with the aid of the  $\delta$  function, leaving an integral over  $v$ . For the lower energy region in Fig. 1(a), where  $-2 - \gamma \leq \varepsilon \leq 2 - \gamma$ , the DOS is obtained as

$$N(E) = N_0 \int_b^a I(v, \varepsilon) dv, \quad (7)$$

where

$$I(v, \varepsilon) = \frac{1}{\sqrt{(a-v)(v-b)(v-c)(v-d)}}, \quad (8)$$

and  $N_0 = 1/(2t_2\pi^2\sqrt{\gamma^2-1})$ , with  $a=1$ ,  $b=-(1+\varepsilon)/(1+\gamma)$ ,  $c=-1$ , and  $d=(\varepsilon-1)/(\gamma-1)$ . In this energy region, we have  $a > b > c > d$ . It is found that such an integral in Eq. (7) can be expressed as a complete elliptic integral of the first kind. Making use of integral formula (3.147) of Ref. 24, we obtain for  $N(E)$  the following expression:

$$N(E) = \frac{1}{2t_2\pi^2\sqrt{1-\gamma\varepsilon}} K\left(\frac{\sqrt{1-(\varepsilon+\gamma)^2/4}}{\sqrt{1-\gamma\varepsilon}}\right). \quad (9)$$

As the modulus of the complete elliptic integral  $K(x)$  is equal to 1,  $K(x)$  exhibits divergent behavior. It is evident that there is no singular point of  $N(E)$  in this region, for the modulus of  $K(x)$  in Eq. (9) is always less than 1. For the middle region in Fig. 1(a), where  $2 - \gamma \leq \varepsilon \leq 1/\gamma$ , we have

$$N(E) = N_0 \left[ \int_b^a I(v, \varepsilon) dv + \int_c^d I(v, \varepsilon) dv \right], \quad (10)$$

where  $a > b > d > c$ . It is easily shown that the two integrals in Eq. (10) are identical to each other and can be also expressed as complete integrals of the first kind, yielding

$$N(E) = \frac{2}{t_2\pi^2(\gamma-\varepsilon)} K\left(\frac{\sqrt{(\varepsilon+\gamma)^2-4}}{\gamma-\varepsilon}\right), \quad (11)$$

where a singular peak appears at  $\varepsilon = 1/\gamma$ . For the upper region in Fig. 1(a), where  $1/\gamma \leq \varepsilon \leq \gamma$ , we have

$$N(E) = N_0 \left[ \int_d^a I(v, \varepsilon) dv + \int_c^b I(v, \varepsilon) dv \right], \quad (12)$$

where  $a > d > b > c$ . Similarly, we obtain

$$N(E) = \frac{2}{t_2\pi^2\sqrt{(\gamma+\varepsilon)-4}} K\left(\frac{\gamma-\varepsilon}{\sqrt{(\varepsilon+\gamma)^2-4}}\right), \quad (13)$$

whose singular peak is also at  $\varepsilon = 1/\gamma$ . According to Eqs. (9), (11), and (13),  $N(2t_2\varepsilon)$  has been drawn as a function of  $\varepsilon$  in Fig. 2 (full line). From these expressions for  $N(E)$  along with Fig. 2, one comes to the following conclusions. First, there is a VHS at  $E = 2t_2/\gamma$ . Taking into account the asymptotic formula  $K(x) \sim \ln[4(1-x^2)^{-1/2}]$  for  $x \approx 1$ , one finds that the DOS near  $E_s = 2t_2/\gamma$  exhibits a logarithmic singularity as  $N(E) \propto \ln(D/|E-E_s|)$  where  $D = 8t_2(\gamma^2 - 1)^2/\gamma^3$ . Since  $8t_2 = 2 \times 1.33J$  is small and  $\gamma$  is very close to unity, the present  $D$  is much smaller than the corresponding value in the 2D tight-binding band calculation.<sup>11</sup> Second, the DOS is small in a wide low-energy region of  $\varepsilon < 2 - \gamma$ ,

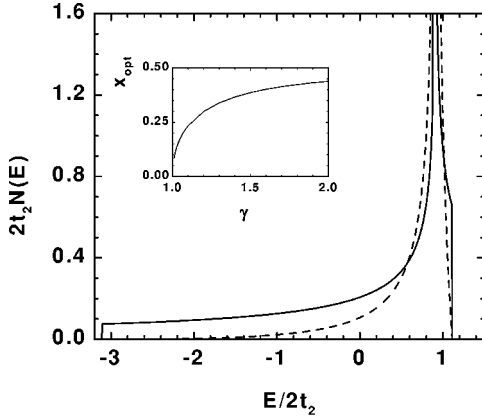


FIG. 2. Electronic DOS  $N(E)$  (solid line) and effective DOS  $N_{eff}(E)$  (dashed line) for  $\gamma=1.113$  (Ref. 19). Both  $N(E)$  and  $N_{eff}(E)$  have the VHS at  $\varepsilon=1/\gamma$ . The inset shows the optimal doping density corresponding to  $E_F=2t_2/\gamma$  as a function of  $\gamma$ .

while there is a large accumulation of weight in DOS in a very narrow energy region between  $\varepsilon=2-\gamma$  and  $\varepsilon=\gamma$ . The two features of DOS above are evidently favorable to the high  $T_c$  of the Cu oxides. Third, it is found from Eqs. (9) and (11) that there is a discrete jump in  $N(E)$  at  $\varepsilon=2-\gamma$ , i.e.,  $N(\varepsilon=2-\gamma+0^+)=K(0)/[t_2\pi^2(\gamma-1)]=2N(\varepsilon=2-\gamma-0^+)$  with  $K(0)=1.5708$ . This jump arises from the fact that the contributions of four vertexes of 2D BZ to the DOS are suddenly added as soon as  $\varepsilon$  exceeds  $2-\gamma$ .

### III. $T_c$ FORMULA AND ISOTOPE COEFFICIENT

For a given class of high- $T_c$  cuprate superconductors, the value of  $T_c$  as a function of dopant level peaks at an optimized composition and decreases with the hole density departing from its optimized value. Another anomaly in the superconducting properties is the very small oxygen-isotope effect for optimized doping and its strong doping dependence. Within the framework of the BCS theory, we consider hole-boson interactions in charge channel as the driving force for the  $d$ -wave pairing:

$$H=V_0\sum_{i\sigma}\mathbf{n}_{i\sigma}\mathbf{n}_{i,-\sigma}-\sum_{\langle i,j\rangle\sigma}V_{ij}\mathbf{n}_{i\sigma}\mathbf{n}_{j,-\sigma}. \quad (14)$$

Here the interactions contain an on-site repulsion ( $V_0>0$ ) and a nearest-neighbor attraction ( $-V_{ij}<0$ ), for example, two holes on adjacent copper sites may experience an attractive interaction due to motion of the intervening oxygen atom. Boson-mediated attractions may provide two attraction channels for  $s$ - and  $d$ -wave pairing.<sup>25</sup> The interactions in the coordinate space can be rewritten as  $V(\mathbf{r}-\mathbf{r}')=V_0\delta(\mathbf{r}-\mathbf{r}')-V_1[\delta(\mathbf{r}-\mathbf{r}'\pm\mathbf{a}_x)+\delta(\mathbf{r}-\mathbf{r}'\pm\mathbf{a}_y)]$  where  $\mathbf{a}_x$  and  $\mathbf{a}_y$  are the unit lattice vector in the  $x$  and  $y$  directions, respectively. The strength of the nearest-neighbor interactions in the  $x$  and  $y$  directions is assumed to be  $-V_1$ . In reciprocal space the attractive interaction  $V(\mathbf{k}-\mathbf{k}')$  is given by

$$V(\mathbf{k}-\mathbf{k}')=V_0-V_1[\cos(k_x-k'_x)+\cos(k_y-k'_y)], \quad (15)$$

where  $a_x=a_y=1$  has been taken.  $V(\mathbf{k}-\mathbf{k}')$  consists of the extended  $s$ -wave,  $d$ -wave, and  $p$ -wave channel interactions.

If the  $p$ -wave channel interaction is neglected since it does not contribute to the spin-singlet pairing state, only  $s$ - and  $d$ -wave channel interactions need to be taken into account and Eq. (15) can be approximately rewritten as

$$V(\mathbf{k}-\mathbf{k}')\simeq-V_s-V_d(\cos k_x-\cos k_y)(\cos k'_x-\cos k'_y), \quad (16)$$

where  $V_s=2V_1-V_0$  and  $V_d=V_1/2$  correspond to the  $s$ - and  $d$ -wave channel interaction constants, respectively. In such a model, both  $V_s$  and  $V_d$  are positive only if  $2V_1>V_0$ . A positive  $V_s$  will give rise to a  $s$ -wave component of the order parameter.<sup>22</sup> For large  $V_0$ ,  $-V_s\geq 0$  so that there is no  $s$ -wave pairing and only  $d$ -wave pairing appears. It follows that for the  $d$ -wave pairing the boson-mediated attractive interactions have the same form as that induced by the AF exchange interactions. Since we focus attention only on the  $d$ -wave pairing, we set  $-V_s\geq 0$  in this work. In this case the order parameter is of the form

$$\Delta(\mathbf{k})=\Delta_d(\cos k_x-\cos k_y). \quad (17)$$

With expressions for  $\Delta(\mathbf{k})$  and  $V(\mathbf{k}-\mathbf{k}')$ , the self-consistent equation for the  $d_{x^2-y^2}$ -wave order parameter is given by

$$1=V_d\int\frac{d\mathbf{k}}{(2\pi)^2}\frac{(\cos k_x-\cos k_y)^2}{2W_{\mathbf{k}}}\tanh\left(\frac{W_{\mathbf{k}}}{2k_B T}\right), \quad (18)$$

where  $W_{\mathbf{k}}^2=\xi_{\mathbf{k}}^2+\Delta_d^2(\cos k_x-\cos k_y)^2$  with  $\xi$  the energy measured relative to  $E_F$ . The critical temperature  $T_c$  is determined by setting  $\Delta_d=0$  in Eq. (18), in which the VHS in DOS plays an important role. In order to compare the VHS effect in the  $d$ -wave pairing case with that in the  $s$ -wave case, we define an effective DOS for the  $d$ -wave pairing as

$$N_{eff}(E)=\frac{1}{\pi^2}\int_0^\pi\int_0^\pi dp_x dp_y (1-\cos p_x)(1-\cos p_y)\times\delta(E-E_{\mathbf{p}}). \quad (19)$$

Here we have used the relation  $(\cos k_x-\cos k_y)^2=(1-\cos p_x)(1-\cos p_y)$  in the integral-variable transformation from  $\mathbf{k}$  into  $\mathbf{p}$ , and the quasiparticle dispersion  $E_{\mathbf{p}}$  has been given in Eq. (2). With the aid of  $N_{eff}(E)$ , the  $T_c$  equation for the  $d$ -wave pairing reduces to

$$1=V_d\int_{-T_{c0}}^{T_{c0}}\frac{d\xi}{2\xi}\tanh\left(\frac{\xi}{2T_c}\right)N_{eff}(\xi+E_F), \quad (20)$$

where the interaction is assumed to be of the charge-coupled type, mediated by bosons, so that the maximum boson energy  $T_{c0}$  (setting  $k_B=1$ ) is used as the cutoff energy of the integral.  $T_c$  formula (20) for the  $d$ -wave pairing has the same form as that in the  $s$ -wave pairing, but the effective DOS in it is quite different from  $N(E)$ . Using the same calculation procedure as in the preceding section,  $N_{eff}(E)$  can be obtained as

$$N_{eff}(E)=N_0\int_b^a I(v,\varepsilon)D(v,\varepsilon)dv \quad (21)$$

for  $\varepsilon\leq 2-\gamma$ ;

$$N_{eff}(E) = N_0 \left[ \int_b^a I(\nu, \varepsilon) D(\nu, \varepsilon) d\nu + \int_c^d I(\nu, \varepsilon) D(\nu, \varepsilon) d\nu \right] \quad (22)$$

for  $2 - \gamma \leq \varepsilon \leq 1/\gamma$ ; and

$$N_{eff}(E) = N_0 \left[ \int_d^a I(\nu, \varepsilon) D(\nu, \varepsilon) d\nu + \int_c^b I(\nu, \varepsilon) D(\nu, \varepsilon) d\nu \right] \quad (23)$$

for  $1/\gamma \leq \varepsilon \leq \gamma$ , with

$$D(\varepsilon, \nu) = \frac{(1 - \nu)[1 + \varepsilon + (1 + \gamma)\nu]}{1 + \gamma\nu}. \quad (24)$$

Here  $a$ ,  $b$ ,  $c$ , and  $d$  as functions of  $\varepsilon = E/(2t_2)$  have given just below Eq. (8). In the  $d$ -wave case,  $N_{eff}(E)$  appeared in the  $T_c$  formula is not a real DOS. Although it cannot be expressed as a simple elliptic integral, its VHS behavior is expected to be similar to  $N(E)$  given in Eqs. (9), (11), and (13). In order to make a comparison between  $N_{eff}(E)$  and  $N(E)$ , we used the same parameter ( $\gamma = 1.113$ ) to calculate them. The calculated results are shown in Fig. 2, where the full and dashed curves represent  $N(E)$  and  $N_{eff}(E)$ , respectively. It is easy to see that both peaks in  $N_{eff}(E)$  and  $N(E)$  have similar divergent behavior at the same energy  $\varepsilon = 1/\gamma$ , but the former appears higher and narrower than the latter. With the energy being away from  $\varepsilon = 1/\gamma$ ,  $N_{eff}(E)$  decreases rapidly and vanishes while  $N(E)$  decreases to a saturated value (about 0.1 in Fig. 2). This feature of  $N_{eff}(E)$  is an important factor of producing a very small  $\alpha$ , as will be shown below. If  $E_F$  is located right at or very close to the VHS,  $N_{eff}(E)$  is concentrated on the vicinity of  $E_F$ . As a result, in the  $d$ -wave case, the average  $N_{eff}(E)$  within the region between  $E_F - T_{c0}$  and  $E_F + T_{c0}$  is large and so favorable to the high- $T_c$  superconductivity.

With effective DOS formulas (21)–(24), the superconducting transition temperature  $T_c$  is determined by Eq. (20). To determine the effect of VHS on the isotope-mass exponent  $\alpha$ , one can differentiate Eq. (20) with respect to  $T_{c0}$ . According to the definition of the isotope shift,  $\alpha = -\partial \ln T_c / \partial \ln M$ , and the relation  $T_{c0} \propto M^{-1/2}$ , the isotope shift for the  $d$ -wave pairing is obtained as

$$\alpha = \frac{1}{2} \frac{N_{eff}(E_F + T_{c0}) + N_{eff}(E_F - T_{c0})}{2\langle N_{eff}(E_F) \rangle} \tanh\left(\frac{T_{c0}}{2T_c}\right), \quad (25)$$

where

$$\langle N_{eff}(E_F) \rangle = \int_{-T_{c0}}^{T_{c0}} \frac{d\xi}{4T_c} N_{eff}(E_F + \xi) \operatorname{sech}^2\left(\frac{\xi}{2T_c}\right). \quad (26)$$

Taking into account that  $\operatorname{sech}^2(x) \approx 1$  for  $x < 1$  and  $\operatorname{sech}^2(x) \approx 0$  for  $x > 1$ , one finds that  $\langle N_{eff}(E_F) \rangle$  is equal to an average of  $N_{eff}(E)$  in the energy range from  $E_F - 2T_c$  to  $E_F + 2T_c$ . It is easily seen that if  $N_{eff}(E)$  were a constant independent of  $E$ , Eq. (25) would reproduce the BCS result:  $\alpha = 1/2$ .

#### IV. RESULTS AND DISCUSSION

In the presence of VHS,  $N_{eff}(E)$  is strongly energy dependent, and a small  $\alpha$  can be achieved for narrow VHS peak, in particular when the half-width of the VHS peak,  $2t_2(\gamma - 1/\gamma)$ , is smaller than  $T_{c0}$ . As  $E_F$  is right at  $E_s = 2t_2/\gamma$ , where  $T_c$  arrives at its maximum, it follows from Fig. 2 that  $N_{eff}(E_F + T_{c0}) = 0$  for  $T_{c0} > 2t_2(\gamma - 1/\gamma)$ , and so  $\alpha$  is proportional to  $N_{eff}(E_F - T_{c0})$  according to Eq. (25). In this case, a small  $N_{eff}(E_F - T_{c0})$  will give rise to  $\alpha$  much smaller than 1/2. As  $E_F$  is away from  $E_s$  to the right,  $N_{eff}(E_F + T_{c0})$  remains vanishing but  $N_{eff}(E_F - T_{c0})$  increases, giving rise to an increase of  $\alpha$ . If  $E_F$  moves towards the left,  $N_{eff}(E_F - T_{c0})$  is very small and  $N_{eff}(E_F + T_{c0}) = 0$  for  $2t_2\gamma - E_F \leq T_{c0}$  so that  $\alpha$  remains its small value. However, as soon as  $2t_2\gamma - E_F$  exceeds  $T_{c0}$ ,  $\alpha$  will increase due to an increase in  $N_{eff}(E_F + T_{c0})$ . For a wide VHS peak,  $\alpha$  is still smaller than 1/2 at optimal doping and it also increases with  $E_F$  away from  $E_s$ . In this case, however, the calculated value of  $\alpha$  is often on the high side compared with its experimental data, as found in the previous VHS model.<sup>4,11</sup>

From the arguments above, the ratio between  $T_{c0}$  and  $2t_2(\gamma - 1/\gamma)$  is an important parameter related to whether a very small  $\alpha$  can be obtained at optimal doping. We wish to point out here that  $\gamma$  appeared in dispersion (1) is not an adjustable parameter but determined by the principle that  $E_F$  is just at  $E_s = 2t_2/\gamma$  for the optimal doping so that there are the highest  $T_c$  and the smallest  $\alpha$ . According to this principle, the optimal doping  $x_{opt}$  is given by

$$x_{opt} = \int_{1/\gamma}^{\gamma} d\varepsilon 2t_2 N(2t_2\varepsilon), \quad (27)$$

where the upper and lower limits are the energies of the band top and the Fermi level, respectively. Since  $2t_2 N(2t_2\varepsilon)$  is independent of  $t_2$ ,  $x_{opt}$  is determined only by  $\gamma$ .  $x_{opt}$  as a function of  $\gamma$  is plotted in the inset of Fig. 2. With increasing  $\gamma$ , the VHS peak moves towards the left and the corresponding  $x_{opt}$  increases. From the inset of Fig. 2, one finds that among several values of  $\gamma$  taken in Refs. 18–20  $\gamma = 1.055$  is a relatively more reasonable value corresponding to  $x_{opt} = 0.15$ .

Figure 3 shows  $\alpha$  at optimal doping as a function of  $T_{c0}/(2t_2)$  for several  $\gamma$ . In the present calculations we have fixed  $2t_2 = 0.083$  eV  $\approx 960$  K (Ref. 19) and  $T_c = 40$  K. Since the variation of  $T_{c0}$  will change  $T_c$ , we keep  $T_c$  unchanged by adjusting the interaction strength  $V_d$  in  $T_c$  formula (20). It is found that  $\alpha$  decreases with increasing  $T_{c0}/(2t_2)$ , decreasing rapidly for  $T_{c0}/(2t_2) < 0.2$  and slowly for  $T_{c0}/(2t_2) > 0.2$ . In the case of narrow VHS peak ( $\gamma = 1.113$  or 1.055),  $\alpha$  has been lower than 0.05 when  $T_{c0}/(2t_2)$  exceeds 0.2, because  $N_{eff}(E_F + T_{c0}) = 0$  and  $N_{eff}(E_F - T_{c0})$  is very small. For wider VHS peak ( $\gamma = 1.53$ ), nonzero  $N_{eff}(E_F + T_{c0})$  makes the value of  $\alpha$  relatively higher. A sudden drop of  $\alpha$  near  $T_{c0}/(2t_2) = 0.2$  stems from the fact that  $N_{eff}(E)$  as well as  $N(E)$  has a big drop at  $\varepsilon = 2 - \gamma$ , being suddenly decreased by half, as has been mentioned in Sec. II. In order to keep  $T_c = 40$  K unchanged in the calculation above,  $v_d$  must be adjusted with the variation of  $T_{c0}$ , as shown in the inset of Fig. 3. In the BCS

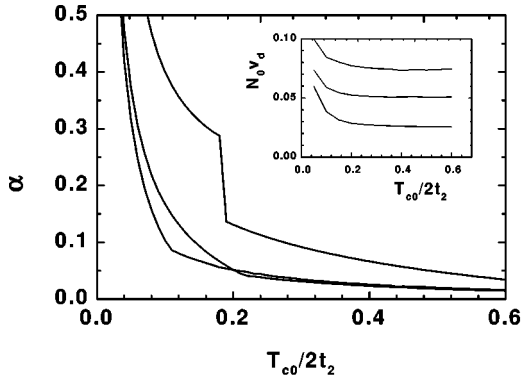


FIG. 3. Calculated results for  $\alpha$  as functions of  $T_{c0}/(2t_2)$  for  $\gamma=1.53, 1.113, 1.055$ , corresponding to the solid lines from up to down (inset, from down to up), respectively, taken in Refs. 18–20. The inset shows the electron-boson interaction  $v_d$  vs  $T_{c0}/(2t_2)$  with  $T_c=40$  K fixed.

theory,  $T_c$  may be enhanced either by increasing  $T_{c0}$  or by increasing  $v_d$ . As a result, a decrease in  $v_d$  can counteract the increase of  $T_{c0}$ , making  $T_c$  constant. As  $T_{c0}/(2t_2) > 0.2$ ,  $v_d$  goes to its saturated value. This is because in this case, the integral range in Eq. (20) has been beyond the region of nonzero  $N_{eff}(E)$  so that the increase of  $T_{c0}$  no longer enhances  $T_c$ . As  $E_F$  is away from  $E_s$ , the hole doping  $x$  departs from the optimal doping  $x_{opt}$ .  $T_c$  and  $\alpha$  as functions of  $x$  are shown in Fig. 4 where  $\gamma=1.055$  and  $T_{c0}=150$  K. In the range of  $0.1 < x < 0.25$ , both the decrease in  $T_c$  and the variation in  $\alpha$  with  $x$  away from  $x_{opt}$  are small. As  $x$  is beyond this range, however,  $\alpha$  increases rapidly accompanied with the decrease of  $T_c$ . This doping dependence of  $\alpha$  is very similar to the result of Ref. 20.

Finally, we wish to point out that unlike the nested-Fermi-liquid theory<sup>26</sup> where there is an ideal nested Fermi surface only at the half filled case, the AFVH model has an ideal nesting of Fermi surface right at optimal doping, as shown in Fig. 1(b). It has been shown<sup>26</sup> that a nested region of Fermi surface can yield an electron-electron scattering rate that is linear in temperature at low frequencies and then becomes

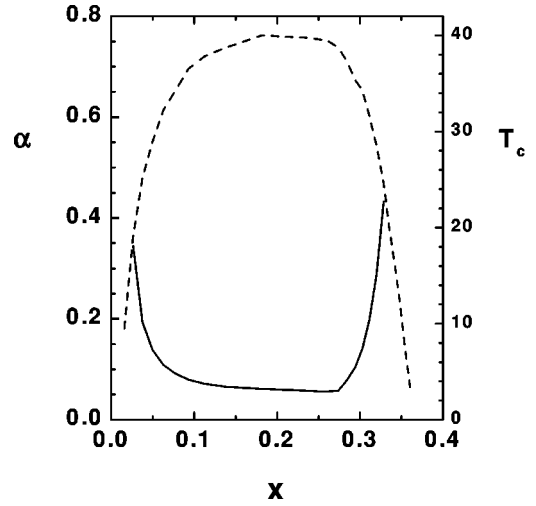


FIG. 4. Calculated results for  $\alpha$  (full line) and  $T_c$  (dashed line) as functions of the hole density  $x$ . The parameters are  $\gamma=1.055$ ,  $T_{c0}=150$  K, and  $v_d/(2t_2)=0.026$ .

linear in frequency  $\omega$  for  $\omega > T$ . Thus the AFVH model is very suitable to accounting for many anomalous normal-state properties of the high- $T_c$  cuprates at optimal doping.

In summary, we have derived analytic expressions for the DOS from the quasiparticle dispersion in an AF background. In the consideration of the  $d$ -wave pairing and hole-boson interactions,  $T_c$  and the oxygen isotope coefficient  $\alpha$  are calculated within the framework of the BCS formalism. The VHS in the DOS always exists in a 2D system, no matter whether the dispersion relation of the quasiparticle is derived from a simple tight-binding band structure or from a strongly correlated electron system. The calculation of the AFVH model yields a very narrow VHS peak in a narrow band, from which a very small  $\alpha$  has been obtained at optimal doping and the doping dependence of  $\alpha$  has been qualitatively reproduced. The physical origin can be understood from the present analytic approach.

This work was supported by the National Natural Science Foundation of China through Grant No. 19874011.

<sup>1</sup>A. J. Freeman, J. Yu, and C. L. Fu, Phys. Rev. B **36**, 7111 (1987); H. Krakauer and W. E. Pickett, Phys. Rev. Lett. **60**, 1665 (1988).

<sup>2</sup>P. A. Lee and N. Read, Phys. Rev. Lett. **58**, 2691 (1988); J. Labbe and J. Bok, Europhys. Lett. **3**, 1225 (1987); J. Friedel, J. Phys.: Condens. Matter **1**, 7757 (1989); R. S. Markiewicz, *ibid.* **2**, 665 (1990).

<sup>3</sup>B. Batlogg, G. Kourouklis, W. Weber, R. J. Cava, A. Jayaraman, A. E. White, K. T. Short, L. W. Rupp, and E. A. Rietman, Phys. Rev. Lett. **59**, 912 (1987); **58**, 2333 (1987); T. A. Falten, W. K. Ham, S. W. Keller, K. J. Leary, J. N. Michaels, A. M. Stacy, H. C. zur Loye, D. E. Morris, T. W. Barbee III, L. C. Bourne, M. L. Cohen, S. Hoen, and A. Zettl, *ibid.* **59**, 915 (1987); L. C. Bourne, M. F. Crommie, A. Zettl, H. C. zur Loye, S. W. Keller, K. L. Leary, A. M. Stacy, K. I. Chang, M. L. Cohen, and D. E. Morris, *ibid.* **58**, 2337 (1987); H. K. Yoshita, T. Hirooka, A. Oyamada, Y. Okabe, T. Takahashi, T. Sasaki, A. Ochiai, T.

Suzuki, A. J. Mascarenhas, J. I. Pankove, T. F. Ciszek, S. K. Deb, P. B. Goldfarb, and Y. K. Li, Physica C **156**, 481 (1989).

<sup>4</sup>C. C. Tsuei, D. M. Newns, C. C. Chi, and P. C. Pattnaik, Phys. Rev. Lett. **65**, 2724 (1990).

<sup>5</sup>M. K. Crawford, M. N. Kunchur, W. E. Farneth, E. M. McCarron, III, and S. J. Poon, Phys. Rev. B **41**, 282 (1990).

<sup>6</sup>J. P. Franck, J. Jung, M. A. K. Mohamed, S. Gyax, and I. G. Sproule, Phys. Rev. B **44**, 5318 (1991).

<sup>7</sup>K. Gofron, J. C. Campuzano, H. Ding, C. Gu, R. Liu, B. Dabrowski, B. W. Veal, W. Cramer, and G. Jennings, J. Phys. Chem. Solids **54**, 1193 (1993); K. Gofron, J. C. Campuzano, A. A. Abrikosov, M. Lindroos, A. Bansil, H. Ding, D. Koelling, and B. Dabrowski, Phys. Rev. Lett. **73**, 3302 (1994); A. A. Abrikosov, J. C. Campuzano, and K. Gofron, Physica C **214**, 73 (1993).

<sup>8</sup>D. S. Dessau, Z. X. Shen, D. M. King, D. S. Marshall, L. W. Lombardo, P. H. Dickinson, A. G. Loeser, J. DiCarlo, C. H.

- Park, A. Kapitulnik, and W. E. Spicer, Phys. Rev. Lett. **71**, 2781 (1993); D. M. King, Z. X. Shen, D. S. Dessau, B. O. Wells, W. E. Spicer, A. J. Arko, D. S. Marshall, J. DiCarlo, A. G. Loeser, C. H. Park, E. R. Ratner, J. L. Peng, Z. L. Peng, and R. L. Greene, *ibid.* **70**, 3159 (1993).
- <sup>9</sup>D. L. Noovikov and A. J. Freeman, Physica C **212**, 233 (1993).
- <sup>10</sup>S. N. Putilin, E. V. Antipov, O. Chmaissem, and M. Marezio, Nature (London) **362**, 226 (1993); A. Schilling, M. Cantoni, J. D. Guo, and H. R. Ott, *ibid.* **363**, 56 (1993).
- <sup>11</sup>D. Y. Xing, M. Liu, and C. D. Gong, Phys. Rev. B **44**, 12 525 (1991); Phys. Rev. Lett. **68**, 1090 (1992).
- <sup>12</sup>S. Sarkar, S. Basu, and A. N. Das, Phys. Rev. B **51**, 12 854 (1995).
- <sup>13</sup>P. C. Pattnaik, C. L. Kane, D. M. Newns, and C. C. Tsuei, Phys. Rev. B **45**, 5714 (1992).
- <sup>14</sup>C. C. Tsuei, C. C. Chi, D. M. Newns, P. C. Pattnaik, and M. Daumling, Phys. Rev. Lett. **69**, 2134 (1992); S. Sarkar and A. N. Das, Phys. Rev. B **54**, 14 974 (1996); S. Dorbolo, M. Ausloos, and M. Houssa, *ibid.* **57**, 5401 (1998).
- <sup>15</sup>D. M. Newns, C. C. Tsuei, R. P. Huchener, P. J. M. van Bentum, P. C. Pattnaik, and C. C. Chi, Phys. Rev. Lett. **73**, 1695 (1994); G. C. McIntosh and A. B. Kaiser, Phys. Rev. B **54**, 12 569 (1996).
- <sup>16</sup>M. Houssa, M. Ausloos, and K. Durczewski, Phys. Rev. B **54**, 6126 (1996).
- <sup>17</sup>Q. P. Li, Physica C **209**, 513 (1993); D. Y. Xing, M. Liu, Z. D. Wang, and J. Dong, Z. Phys. B **100**, 191 (1996).
- <sup>18</sup>E. Dagotto, A. Nazarenko, and M. Boninsegni, Phys. Rev. Lett. **73**, 728 (1994); E. Dagotto, Rev. Mod. Phys. **66**, 763 (1994).
- <sup>19</sup>E. Dagotto, A. Nazarenko, and A. Moreo, Phys. Rev. Lett. **74**, 310 (1995).
- <sup>20</sup>A. Nazarenko and E. Dagotto, Phys. Rev. B **53**, R2987 (1996).
- <sup>21</sup>D. M. Newns, C. C. Tsuei, and P. C. Pattnaik, Phys. Rev. B **52**, 13 611 (1995).
- <sup>22</sup>M. Liu, D. Y. Xing, and Z. D. Wang, Phys. Rev. B **55**, 3181 (1997); M. Liu, H. Y. Teng, D. Y. Xing, and J. Dong, Physica C **282-287**, 1649 (1997).
- <sup>23</sup>A. L. Fetter and J. D. Walecka, *Quantum Theory of Many-Particle Systems* (McGraw-Hill, New York, 1971).
- <sup>24</sup>I. S. Gradshteyn and I. M. Ryzhik, *Table of Integrals, Series, and Products* (Academic Press, London, 1980).
- <sup>25</sup>J. H. Xu, Y. Ren, and C. S. Ting, Phys. Rev. B **52**, 7663 (1995); Y. Ren, J. H. Xu, and C. S. Ting, *ibid.* **53**, 2249 (1996).
- <sup>26</sup>A. Virosztek and J. Ruvalds, Phys. Rev. B **42**, 4064 (1990).